



**HAL**  
open science

# Assessment of Finite Element Simulation Methodologies for the Use of Paschen's Law in the Prediction of Partial Discharge Risk in Electrical Windings

Theo Mathurin, Stephane Duchesne, Guillaume Parent

## ► To cite this version:

Theo Mathurin, Stephane Duchesne, Guillaume Parent. Assessment of Finite Element Simulation Methodologies for the Use of Paschen's Law in the Prediction of Partial Discharge Risk in Electrical Windings. IEEE Access, 2020, 8, pp.144557-144564. 10.1109/ACCESS.2020.3013337 . hal-03198909

**HAL Id: hal-03198909**

**<https://univ-artois.hal.science/hal-03198909>**

Submitted on 15 Apr 2021

**HAL** is a multi-disciplinary open access archive for the deposit and dissemination of scientific research documents, whether they are published or not. The documents may come from teaching and research institutions in France or abroad, or from public or private research centers.

L'archive ouverte pluridisciplinaire **HAL**, est destinée au dépôt et à la diffusion de documents scientifiques de niveau recherche, publiés ou non, émanant des établissements d'enseignement et de recherche français ou étrangers, des laboratoires publics ou privés.

Received April 24, 2020

Digital Object Identifier 10.1109/ACCESS.2020.xxxxxx

# Assessment of finite element simulation methodologies for the use of Paschen's law in the prediction of partial discharge risk in electrical windings

THÉO MATHURIN<sup>1</sup>, STÉPHANE DUCHESNE<sup>1</sup>, AND GUILLAUME PARENT<sup>1</sup>

<sup>1</sup>Univ. Artois, UR 4025, Laboratoire Systèmes Électrotechniques et Environnement (LSEE), Béthune, F-62400, France

Corresponding author: guillaume.parent@univ-artois.fr

The authors acknowledge the support of SafranTech.

**ABSTRACT** The prediction of partial discharge (PD) occurrence in electrical motors at the design phase is key to the development of future devices. As a result, there is a growing interest for predictive numerical tools to help assess partial discharge risk. Currently, most efforts rely on Paschen's law as a criterion for partial discharge occurrence between two neighboring wires. Its use requires field lines data obtained with finite element electrostatic simulations. In this paper, we explore the extent to which these finite element simulations can be simplified without losing accuracy regarding subsequent partial discharge risk assessment using Paschen's law. First, we examine whether partial discharge risk predictions between two turns are influenced by the presence of other turns nearby. Our results suggest that the partial discharge is mostly a local phenomenon hardly affected by the surroundings. Performing simulations for an isolated pair of conductors may thus be sufficient to determine the maximum allowable constraints between two turns, at least for large wires. Also, we show that neglecting field line curvature in the calculation does not alter predictions, vindicating the straight line assumption which has been adopted in the literature for the sake of simplicity.

**INDEX TERMS** partial discharges, electric motors, finite element analysis, insulation testing

## I. INTRODUCTION

Current trends in the electrical engineering industry lead to increasingly severe stresses on the windings of inverter-fed motors [1,2]. This is in part due to the increase in bus voltages to achieve higher power density and to the impact of steep voltage fronts typical of pulse width modulation power supplies. The propagation of these fronts amplified by the impedance mismatch between power cable and winding results in uneven distributions of voltages within windings [3], and therefore high transient voltages between neighboring turns that can generate partial discharges (PDs) [4,5]. It has been largely reported in the literature that the occurrence of PDs in windings can play a key role in the premature aging of insulation systems and can eventually lead to electrical failure [1,6]. As a result, there is a growing interest for predictive tools that would allow manufacturers to know at the design phase if a motor would be at risk of damage from PDs during operation.

There have been several efforts to numerically assess partial discharge risk in electrical windings [7]–[13]. So far, most attempts have relied on Paschen's law [14]–[16] as a criterion for PD risk assessment. For any value of the product  $p \times d$  (gas pressure times distance), this law provides an analytical threshold voltage above which there is a risk of discharge between two electrodes. Although originally devised for uniform and stationary electric fields, Paschen's law is routinely used in the context of electrical windings [7]–[12]. This has overall led to satisfactory prediction results despite lingering concerns over its validity in some circumstances, such as high pressure [17] or very small gap lengths [18]–[20].

In order to draw a comparison with Paschen's threshold voltage, the computation of the length of field lines in the region studied, as well as the corresponding voltage drops, is necessary. Considering the geometry, finite element electrostatic simulations are required to obtain these data. Overall,

all authors follow the same general approach, although the methodologies proposed vary in two important respects.

First, simulations can be carried out at different scales. Most authors have focused on twisted or parallel pairs of enameled wires [7]–[10,12,13,21]. The PD inception voltage (PDIV) predictions reported are in good agreement with experimental results. However, it remains to be seen whether results obtained on an isolated pair can be transposed to PDs occurring between wires inside an actual winding, as it effectively amounts to the assumption that the impact of the rest of the winding can be discounted. Meanwhile, simulations have also been carried out more recently at the scale of a whole winding in a slot [11].

Second, two options have been explored to determine the length of field lines between two wires. The most straightforward way is to consider them as straight lines and neglect their curvature [7,9,12]. In addition to the error on line length that it entails, the use of this strong assumption is restricted to symmetrical cases. For these reasons, authors have put forward different methods to compute actual field line lengths. One of them involves a simulation based on a scalar potential formulation followed by an *ad-hoc* reconstruction of field lines [11], which constitutes a numerically intensive post-processing. An alternative is to follow a two-step numerical approach [8,22], combining a vector potential formulation, which allows to retrieve field lines, with a scalar formulation providing the corresponding voltage drops. The use of the vector formulation comes with a simplified post processing, but may become laborious depending on the topology of the problem studied [23].

In this paper, we explore the extent to which the finite element simulations and post-processing needed to carry out PD risk assessment with Paschen's criterion can be simplified without a loss in prediction accuracy. For this purpose, we seek to quantitatively examine the relative relevance of the methodological choices found in the literature, as mentioned above. This will shed light on the minimal simulation and post-processing requirements that are necessary to use Paschen's law in the context of partial discharge risk prediction in the windings of electrical machines.

In a first investigation we check what influence, if any, the surroundings exert on PDs occurring between two turns. For this purpose, we assess in what way the risk of PD between two wires is modified by the presence of a third wire of intermediate electrical potential in contact with them. Then, we look into the validity of the straight line assumption and its influence on PDIV prediction. In section II, we present the methodology adopted whereas in section III, we present the corresponding results, draw the main conclusions from them and address some important caveats. We then propose a revised outlook on numerical predictions of PD risk based on our results.

## II. METHODOLOGY

### A. OVERVIEW

The general aim of a predictive tool for PD risk assessment at the design phase is the determination of the maximum electrical constraints that the stator windings of a prospective motor can bear without damage. When increasing the severity of turn-to-turn constraints, PDs will first occur during operation between the two neighboring turns associated with the largest transient voltage drop.

However, it is not known whether carrying out simulations on an isolated pair of wires accurately reflects the behavior of the same pair embedded in a stator winding. Indeed the situation in a winding is more complex as the electric potential of surrounding conductors and the proximity of the stator iron may all affect the electric field distribution in the region where PDs will appear. It follows that in principle an impact on PD activity cannot be discounted.

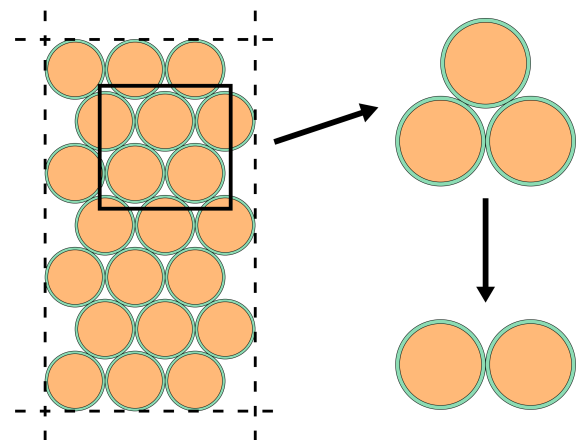


**FIGURE 1.** It is not known whether the prediction of PD risk for a pair of wires can accurately reflect that of an entire winding. Looking at the influence of a third conductor can bring valuable information.

In the search for the minimal study domain required for accurate prediction we can start from the simplest pattern, *i.e.* the plain pair of conductors, and gradually add complexity to see if results are affected in any way. As a first step, it is thus natural to look at the influence of a third conductor nearby. The main metric will be the minimum voltage needed for the inception of PDs (PDIV) between two turns using Paschen's criterion. The PDIV stands as a relevant indicator to assess partial discharge risk [24].

The other unknown we wish to address is the relevance of the straight line assumption found in the literature [7]–[10]. Indeed, for a given pair of field line extremities on the insulation surface of two wires—and thus a given voltage drop—line length is systematically underestimated. Authors have argued that the error is negligible for such small lengths [9,25]. Here, we seek to quantify that error, both relative to the length itself but also to the impact on PDIV prediction.

Note that this work focuses on round enameled wires so that the analysis and conclusions do not apply to other geometries such as rectangular conductors.

## B. NUMERICAL METHOD

The electrostatic simulations are run on a two-dimensional mesh domain comprising two identical insulated conductors, labeled 1 and 2, in contact with each other and surrounded by air (permittivity  $\epsilon_0$ ). The conductors are put to an electric potential of 0 and 1 V respectively, while a zero potential Dirichlet boundary condition is imposed on the outer air domain boundary. Simulations are performed both with and without a third wire of identical dimensions in contact with wires 1 and 2, forming a closed air gap in a way that is fairly representative of real wire arrangements in a winding (see Fig. 1). In order to explore the electrostatic influence of conductor 3, for any given geometry simulations have been carried out with its electric potential varying from 0 V to 1 V. By setting an intermediate potential on conductor 3, the largest voltage drops will be between wires 1 and 2 so that PDs are supposed to occur between these two. The simulations performed in the absence of a third wire can be used as a reference and will also allow us to test the validity of the straight line assumption.

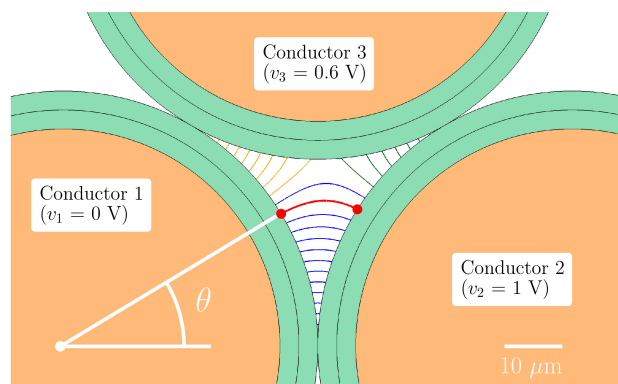


**FIGURE 2.** Calculated field lines in an air gap between three wires (wire radius is  $40 \mu\text{m}$ , insulation thickness is  $7 \mu\text{m}$ ), with a potential of  $0.6 \text{ V}$  imposed on conductor 3. The field line and corresponding angle  $\theta$  where PDs are predicted to occur are highlighted. The voltage drop is calculated between the two red dots on the insulation surface.

The method hereby followed to determine PDIV is similar to what has been presented previously [22]. The electrostatic simulation run is two-fold. The first step consists in solving the electrostatic problem by means of the electric scalar potential, denoted  $v$ , formulation:

$$\text{div}(\epsilon \text{ grad } v) = \rho \quad (1)$$

where  $\epsilon$  is the permittivity,  $\rho$  is the charge density and  $v$  is related to the electric field, denoted  $e$ , through its gradient such that  $e = -\text{grad } v$ . Then, this computation allows to obtain the distribution of  $v$  within the studied domain and in particular on each insulation surface boundary. The second step consists in solving the same electrostatic problem by means of the electric vector potential, denoted  $u$ , formulation:

$$\text{curl}(\epsilon^{-1} d_s) + \text{curl}(\epsilon^{-1} \text{curl } u) = \rho \quad (2)$$

where  $e = \text{curl } u$  and  $d_s$  is a source field ensuring  $\text{div } d_s = \rho$  such that  $d_s$  and  $u$  are related to the electric induction, denoted  $d$ , as follows [22,23,26]:

$$d = d_s + \text{curl } u \quad (3)$$

Then, this computation allows to obtain the distribution of  $u$  within the studied domain and in particular in the air region. As previously stated, the simulations are run on a two-dimensional mesh domain, which leads to  $u = u z$  where  $z$  is the unit vector perpendicular to the studied plane. Thus, the electric field can be written as  $e = \epsilon^{-1} \text{curl } u = \epsilon^{-1} (\text{grad } u) \times z$  which implies that the field lines are the iso- $u$  lines. A dedicated script then extracts an arbitrary number of field lines starting from a set of points equally distributed on the outer insulation boundary of wires, with a precision of 20 field lines per degree. Field lines can then be identified either by their number or the corresponding  $\theta$  angle with respect to the equator of wire 1 (see Fig. 2).

It is then possible to compute the length of each field line and the associated voltage drops. When gathering data for all field lines, a curve can be plotted and compared with Paschen's curve, see Fig. 3 for an example. Because the studied problem is completely linear, if the voltage imposed between conductor 1 and conductor 2 is multiplied by a given factor, all voltage drops will be multiplied by the same factor, so that all curves will be shifted upwards. Thus by definition the predicted PDIV is equal to the multiplication factor we need to apply to voltage drops in order to obtain tangency with Paschen's curve. The point closest to Paschen's curve corresponds to the field line where PDs are first predicted to occur when the input voltage is gradually increased. Note that Paschen's curve is here calculated at a fixed pressure of  $101\,325 \text{ Pa}$ , used throughout this study.

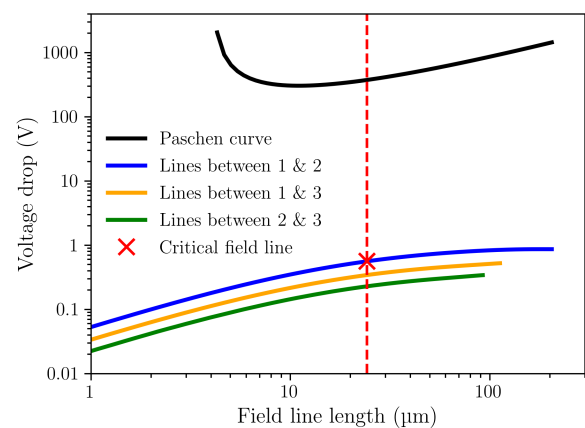


**FIGURE 3.** Voltage drop and Paschen's curve plotted against field line length, in the case of three conductors, here with a potential of  $0.6 \text{ V}$  imposed on conductor 3 as an example (wire radius is  $0.4 \text{ mm}$ , insulation is  $28 \mu\text{m}$  thick). The curve corresponding to lines between wires 1 and 2 is always above the others, because of higher applied voltage. This confirms that PDs will preferentially appear between these two. The point corresponding to the critical line is highlighted.

Separately, we can also look at the error made when field line curvature is neglected, first by quantifying the underestimation of field line length itself, and then by considering straight line length in the calculation of PDIV described above.

In order to build a more comprehensive understanding, we ran simulations for all wire sizes and insulation grades found in the IEC standard for enameled wires [27]. Also, for a conductor of given size and grade, we considered both the lower and upper limits of insulation thickness. As for the insulation material, we simulated a double layer constituted of two polymers of identical thickness. Relative permittivities ( $\epsilon_r$ ) typical of polymers used in enameled wires were set (4.5 for the layer in contact with the conductor, and 2.4 for the one on the outside).

### III. RESULTS

#### A. IMPACT OF THIRD CONDUCTOR

As a first step, let us examine the threshold voltage needed to induce PDs in a pair of conductors undisturbed, which will then be used as a reference. Results are shown in Fig. 4.

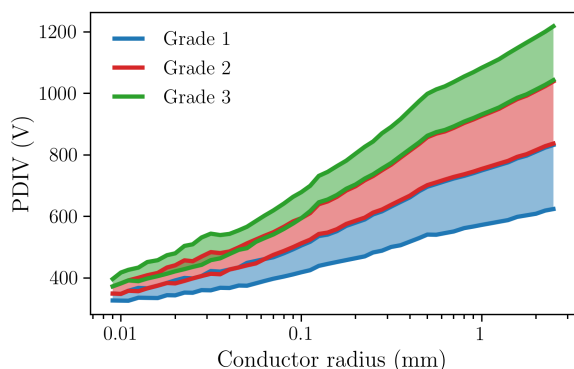


FIGURE 4. Predicted PDIV for all insulation grades in the absence of a third wire.

The remarkable increase in PDIV with increasing radius is in part related to a corresponding increase in insulation thickness. These results also show a quite large variation of PDIV for a given radius and insulation grade, due to the large range of insulation thickness for any given wire size and grade. One can notice some overlap between the different grades, which is directly related to overlaps in insulation thickness between grades in the IEC standard [27].

Now, in the presence of a third wire there will be one prediction of PDIV calculated for each value of electric potential imposed on conductor 3. Because of symmetry considerations, we expect to obtain the whole range of results by covering potentials between 0 V and 0.5 V. Indeed since only differences in potentials matter, when a potential of  $v_0$  is imposed on conductor 3, we effectively have the same turn-to-turn constraints as if we set it to  $1 - v_0$ , with conductor 1 and 2 switching roles. We ascertained that in these symmet-

rical cases the PDIV, the lengths of the field lines as well as the associated voltage drops were all unchanged.

The following figures only show data relative to grade 2 insulation for the sake of visual clarity. The results for other grades being completely analogous, choosing one grade over another has no incidence on the content of the ensuing discussion.

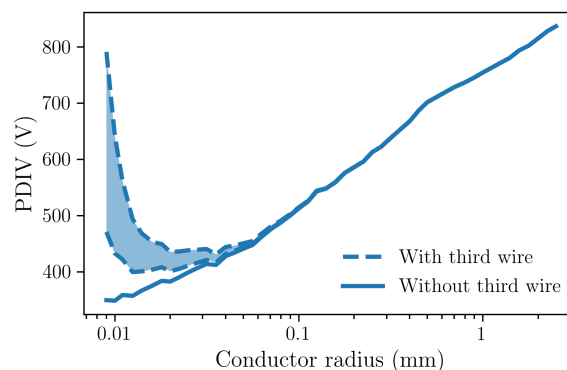


FIGURE 5. Comparison of predicted PDIV with and without third conductor. The range between blue dashed lines reflects the range of PDIV values obtained for various potentials imposed on conductor 3. As the radius increases, this range vanishes and is reduced to a single value in good agreement with the reference PDIV prediction. For the sake of readability, only results obtained with minimum insulation thickness are shown.

In Fig. 5, predicted PDIV values in the presence of a third wire are superimposed with the reference case. We can see that there is little to no difference for conductors with radii larger than 0.1 mm, whereas a large deviation from the reference can be seen for smaller radii. This deviation is due to the fact that PDs between wires 1 and 2 are predicted to occur along field lines which paths draw near to the third wire where its electrostatic influence is felt (see Fig. 2 where the radius is 40  $\mu\text{m}$  for instance). For the smallest radii, the mere presence of the third wire even precludes the existence of the longer lines seen in the reference case.

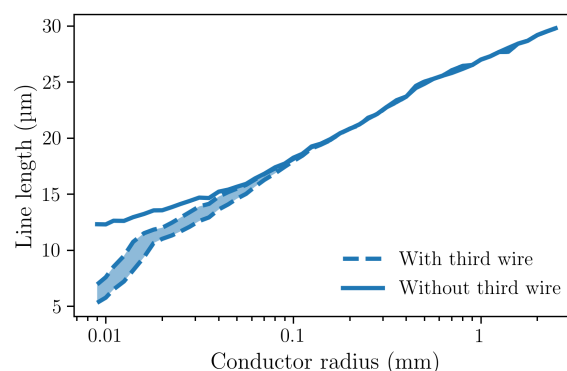


FIGURE 6. Length of field line where PD occurs. Again the range of results obtained for different potentials on wire 3 is quickly reduced to a single value as the radius increases. For the sake of readability, only data obtained with minimum insulation thickness are shown.

It should be noted that, as it has been reported that Paschen's law yields poor results in the case of very small air gaps [18]–[20], PDIV predictions associated with smaller radii are not reliable. And indeed Fig. 6 shows that the field lines identified using Paschen's criterion in the presence of wire 3 are shorter than in the reference case, with lengths as low as a few micrometers. Given that the threshold voltage located left of the Paschen minimum is greatly overestimated [19], the increase in PDIV for smaller radii seen in Fig. 5 is doubtful, but the electrostatic influence of wire 3 is nonetheless established.

As the radius increases however, PDs are predicted to occur closer to the equator ( $\theta = 0$ , see Fig. 2) and the risk of PD is therefore less and less influenced by the presence of the third wire. Our data also show that whatever the potential of conductor 3, the predicted PD field line remains the same and its location remains unchanged (with a margin of error of one-tenth of a degree). Further, there is a good agreement with the reference case, *i.e.* in the absence of wire 3, in both PD location and field line length. In other words, in our simulations the electric potential and even the presence of a third wire has no influence on PD risk or PD location for larger wires.

These results suggest that the overall influence of surroundings may be neglected without any loss of accuracy for wire radii roughly superior to 0.1 mm, and that in these cases the predicted PD behavior of a pair of conductors is unchanged when put into a winding. Indeed, since even a conductor in the immediate vicinity exerts no influence, it is all the more certain that other conductors, located even farther from the PD region, will not matter as their electrostatic influence will be even weaker. The same reasoning applies to the proximity of the stator iron. In other words, in the context of electrical motors, the predicted PD risk in an isolated pair accurately reflects that of a pair inside a winding, so that simulations at the scale of entire windings seem unnecessary.

### B. VALIDITY OF THE STRAIGHT LINE ASSUMPTION

The impact of neglecting field line curvature can first be assessed by directly quantifying the underestimation of the length for the field line where PDs are predicted to occur. Fig. 7 shows that the error is quite substantial for small wires—as much as 15%—but quickly becomes negligible for larger wires. This is because the line gets gradually closer to the equator as the radius increases, as shown in the same figure, so that its curvature vanishes. As an aside, large field line angles  $\theta$  for small radii are also the reason why the presence of a third conductor had some influence, as discussed in the previous subsection. In any case, beyond a radius of 1 mm, the error in line length is below 1%.

The second, and arguably more important check consists in looking at the outcome of PDIV predictions when the calculation is performed with the length of straight lines instead of real field lines. For a given voltage drop on the insulation surface, the length will be slightly smaller when neglecting field line curvature. Therefore on a plot like in

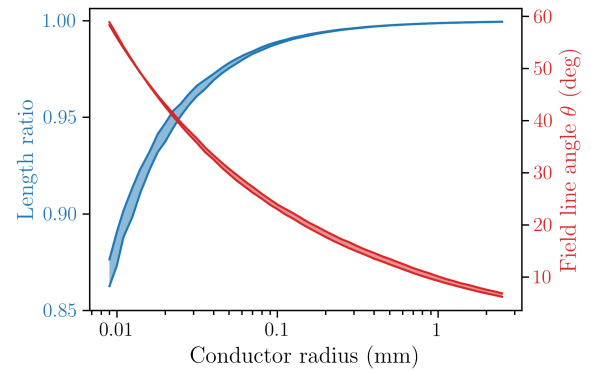


**FIGURE 7.** Straight line to real field line length ratio (blue) and angle of field line starting point  $\theta$  (red), illustrated in Fig. 2. The length discrepancy is quite substantial for smaller radii but gradually decreases as the predicted PD location gets closer to the equator. For the sake of visual clarity, only results for grade 2 are shown. The range on values corresponds to the range of insulation thickness.

Fig. 3, the straight line assumption will cause a shift of the curves towards the left. It follows that a different point will be the closest to Paschen's curve and thus a different PDIV prediction will be found.

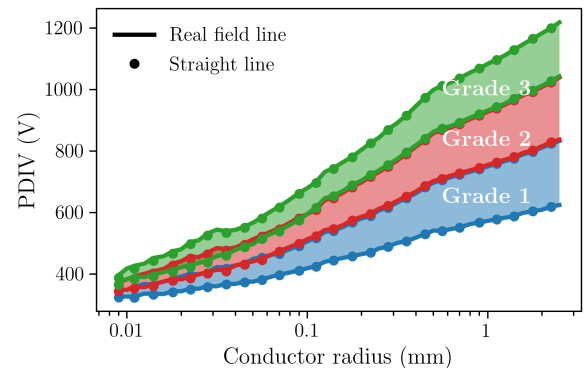


**FIGURE 8.** Comparison of PDIV with straight lines and actual field line lengths for all insulation grades. The agreement is very good for all grades, even for small wires.

As shown in Fig. 8, the agreement with respect to PDIV prediction is very good nonetheless and even extends to small radii despite the substantial curvature of field lines. This is because the closest point to Paschen's curve will correspond to a straight line farther from the equator. All in all, the length of the identified straight line and the associated voltage drop are very close to what is found without the straight line assumption, as shown on Fig. 9. For larger wire sizes, the PD location predicted with straight lines is also the same as that predicted with real field lines, as their curvature vanishes.

These results suggest that, from the point of view of PDIV prediction, the straight line assumption yields reliable results, even in the case of fairly curved field lines for small radii.

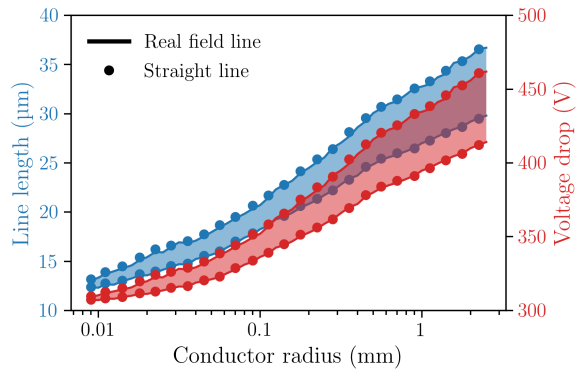


**FIGURE 9.** Prediction of voltage drop and line length with straight line assumption and real field line calculation for grade 2 wires. Upper and lower values correspond to thicker and thinner insulation thickness, respectively.

### C. DISCUSSION

The lack of influence of a third wire located in the immediate vicinity of the PD region for sufficiently large conductor radii is a remarkable result. As stated previously, this lends support to the idea that the electrostatic influence of the rest of the winding can be neglected in the determination of the turn-to-turn constraints needed to induce PDs between two wires.

This means that for a given set of environmental conditions (temperature, humidity...), this threshold voltage is mostly determined by the characteristics of the wire considered and is independent of the specifics of the winding and voltage distribution within it. In this way, it could be viewed as an intrinsic property of the wire that could in principle be provided by wire manufacturers like other quantitative parameters such as the dielectric loss factor, based on standard experimental measurements. In any case, it could be estimated numerically at remarkably low computational cost (seconds), provided that the relevant parameters are known. In particular, precise knowledge of insulation thickness is key, as we have shown that the range of thickness allowed for a given grade translates to large variations in PD behavior. Also, it is important to use appropriate values in terms of relative permittivity for the insulation material and other physical parameters such as the secondary electron emission coefficient involved in Paschen's law [28].

Our investigation on the validity of the straight line assumption vindicates an approach already adopted in the literature but the impact of which had not been properly studied as of yet. This approximation further reduces the computational demands required as ultimately the determination of electric field lines proved unnecessary in practice. Only one scalar electric potential finite element simulation is needed to obtain the voltage drops, with only limited post-processing. However, one should keep in mind that it can only be used when the system studied is symmetrical. Indeed, it is necessary to know where the extremities of field lines are located on the insulation surface in order to obtain the lengths of the corresponding straight lines. The determination

of actual field lines would still be required in the case of more complex geometries, such as wires of different sizes or busbars.

Insofar as we used Paschen's law as a criterion for PD risk throughout our analyses, our conclusions are in principle only as reliable as Paschen's law itself. Doubts on its validity at small length scales prompt considerable caution as regards to the results obtained on very small gaps. However this mostly affects wires with very small conductor radius that are usually not used in motor windings. Strictly speaking, if another criterion such as a modified version of Paschen's law or the streamer inception criterion would prove superior in terms of PDIV predictions, the same investigations would have to be carried out to test the robustness of our conclusions. Nonetheless, beyond the choice of Paschen's law as a criterion, in many cases the agreement with the reference is just a consequence of the close agreement in the underlying data, be it between the potential distribution with and without wire 3 or between the straight line and real field line length in the PD region. As an aside, it has been reported in the literature [9,29] that partial discharge inception occurs at lower voltage levels for slowly-varying sinusoidal excitation than for PWM-like excitation, indicating that the use of Paschen's model may yield conservative predictions.

Finally from an operational point of view, what matters most is the PDIV relative to the winding or motor, *i.e.* the threshold regarding the supply voltage. However it is not straightforward to infer the critical supply voltage of a winding from the turn-to-turn constraints needed to induce PDs. The knowledge of the constraints between turns requires the calculation of the transient electrical response of the winding, fed with a given voltage source, and the distribution of voltage within it. Numerical tools designed for that purpose have already been described in the literature [30,31]. One can then estimate the risk of PDs and their location in the winding by comparing the simulated turn-to-turn voltages with the predicted threshold obtained with a simulation on a pair of conductors. It thus seems possible to build a comprehensive, integrated numerical tool to predict the risk of PDs in motor windings at the design phase with only limited computational effort.

### IV. CONCLUSION

In this study we explored the extent to which the numerical prediction of PD risk in a winding can be simplified without incurring a loss in accuracy. Our conclusions only apply to round wires with radii beyond 0.1 mm, which is not restrictive since smaller radii are seldom used in motor windings.

Our results suggest that the onset of PDs is a local phenomenon that mostly depends on the geometry and insulation materials of the wire considered. They also show that the curvature of field lines can be neglected in the calculation. The synthesis of these two investigations sheds a new light on the minimal procedure required to predict the allowable turn-to-turn constraints in an arbitrary winding using Paschen's criterion. Indeed, it seems sufficient to carry out one scalar

electrostatic simulation on a pair of wires to obtain voltage drops, along with a fairly simple post-processing involving a calculation with straight line lengths. The results obtained at greatly reduced computational effort can then apply for any winding for which detailed transient voltage distribution during operation is known. We argue that this work improves the prospects for current endeavors to devise numerical predictive tools for PD risk assessment.

## REFERENCES

- [1] G. Stone, I. M. Culbert, and B. Lloyd, "Stator insulation problems associated with low voltage and medium voltage PWM drives," in Proc. Cement Indus. Tech. Conf., Charleston, SC, USA, Apr. 2007, pp. 187–192.
- [2] C. Abadie, T. Billard, and T. Lebey, "Partial discharges in motor fed by inverter: from detection to winding configuration," IEEE Trans. Ind. Appl., vol. 55, no. 2, pp. 1332–1341, Mar. 2019, DOI: 10.1109/TIA.2018.2874875.
- [3] P. Bidan, T. Lebey, G. Montseny, and J. Saint-michel, "Transient voltage distribution in inverter fed motor windings: experimental study and modeling," IEEE Trans. Power Electron., vol. 16, no. 1, pp. 92–100, Jan. 2001, DOI: 10.1109/63.903993.
- [4] G. Stone and V. Warren, "Objective methods to interpret partial-discharge data on rotating-machine stator windings," IEEE Trans. Ind. Appl., vol. 42, no. 1, pp. 195–200, Jan. 2006, DOI: 10.1109/TIA.2005.861273.
- [5] P. Wang, G. C. Montanari, and A. Cavallini, "Partial discharge phenomenon and induced aging behavior in rotating machines controlled by power Electronics," IEEE Trans. Ind. Electron., vol. 61, no. 12, pp. 7105–7112, Dec. 2014, DOI: 10.1109/TIE.2014.2320226.
- [6] M. Kaufhold, G. Borner, M. Eberhardt, and J. Speck, "Failure mechanism of the interturn insulation of low voltage electric machines fed by pulse-controlled inverters," IEEE Electr. Insul. Mag., vol. 12, no. 5, pp. 9–16, Sep. 1996, DOI: 10.1109/57.537190.
- [7] N. Hayakawa and H. Okubo, "Partial discharge characteristics of inverter-fed motor coil samples under AC and surge voltage conditions," IEEE Electr. Insul. Mag., vol. 21, no. 1, pp. 5–10, Jan. 2005, DOI: 10.1109/MEI.2005.1389265.
- [8] S. Duchesne, G. Parent, J. Moenclay, and D. Roger, "Prediction of PDIV in motor coils using finite element method," in Proc. ICD, Montpellier, France, Jul. 2016, pp. 638–641, DOI: 10.1109/ICD.2016.7547696.
- [9] L. Benmamas, P. Teste, G. Krebs, E. Odic, F. Vangraefschepe, and T. Hamiti, "Contribution to partial discharge analysis in inverter-fed motor windings for automotive application," in Proc. EIC, Baltimore, MD, USA, Jun. 2017, pp. 348–351, DOI: 10.1109/EIC.2017.8004701.
- [10] N. Driendl, F. Pauli, and K. Hameyer, "Modeling of partial discharge processes in winding insulation of low-voltage electrical machines supplied by high du/dt inverters," in Proc. IECON, Lisbon, Portugal, Oct. 2019, pp. 7102–7107, DOI: 10.1109/IECON.2019.8926661.
- [11] P. Collin, D. Malec, and Y. Lefevre, "A general model to compute the electric flux lines in the slots of electric machines for the evaluation of partial discharge risk," in Proc. COMPUMAG, Paris, France, Jun. 2019.
- [12] V. Madonna, P. Giangrande, W. Zhao, H. Zhang, C. Gerada, and M. Galea, "On the Design of Partial Discharge-Free Low Voltage Electrical Machines," in Proc. IEMDC, San Diego, CA, USA, May 2019, pp. 1837–1842, DOI: 10.1109/IEMDC.2019.8785413.
- [13] L. Lusuardi, A. Cavallini, M. G. de la Calle, J. M. Martínez-Tarifa, and G. Robles, "Insulation design of low voltage electrical motors fed by PWM inverters," IEEE Electr. Insul. Mag., vol. 35, no. 3, pp. 7–15, May 2019, DOI: 10.1109/MEI.2019.8689431.
- [14] F. Paschen, "Ueber die zum Funkenübergang in Luft, Wasserstoff und Kohlensäure bei verschiedenen Drucken erforderliche Potentialdifferenz," Annalen der Physik, vol. 273, no. 5, pp. 69–96, 1889, DOI: 10.1002/andp.18892730505.
- [15] T. W. Dakin, "Breakdown of gases in uniform fields – Paschen curves for nitrogen, air and sulfur hexafluoride," Electra, vol. 32, pp. 61–82, 1974, CIGRE Study Committee 15.
- [16] M. A. Lieberman and A. J. Lichtenberg, Principles of plasma discharges and materials processing, 2nd ed. Hoboken, NJ, USA: John Wiley & Sons, Inc., 2005, DOI: 10.1002/0471724254.
- [17] F. L. Jones and C. G. Morgan, "Failure of Paschen's Law and Spark Mechanism at High Pressure," Physical Review, vol. 82, no. 6, pp. 970–971, Jun. 1951, DOI: 10.1103/PhysRev.82.970.
- [18] D. B. Go and D. A. Pohlman, "A mathematical model of the modified Paschen's curve for breakdown in microscale gaps," Journ. of Appl. Phys., vol. 107, no. 10, p. 103303, May 2010, DOI: 10.1063/1.3380855.
- [19] A. Peschot, N. Bonifaci, O. Lesaint, C. Valadares, and C. Poulain, "Deviations from the Paschen's law at short gap distances from 100 nm to 10  $\mu$ m in air and nitrogen," Appl. Phys. Lett., vol. 105, no. 12, p. 123109, Sep. 2014, DOI: 10.1063/1.4895630.
- [20] A. M. Loveless and A. L. Garner, "Universal gas breakdown theory from microscale to the classical paschen law," in Proc. ICOPS, May 2017, pp. 1–1, OI: 10.1109/PLASMA.2017.8496086.
- [21] G. C. Montanari and P. Seri, "About the Definition of PDIV and RPDIV in Designing Insulation Systems for Rotating Machines Controlled by Inverters," in Proc. EIC, Jun. 2018, pp. 554–557, DOI: 10.1109/EIC.2018.8481069.
- [22] G. Parent, M. Rossi, S. Duchesne, and P. Dular, "Determination of partial discharge inception voltage and location of partial discharges by means of paschen's theory and FEM," IEEE Trans. Magn., vol. 55, no. 6, pp. 1–4, Jun. 2019, DOI: 10.1109/TMAG.2019.2902374.
- [23] G. Parent, S. Duchesne, and P. Dular, "Determination of flux tube portions by adjunction of electric or magnetic multivalued equipotential lines," IEEE Trans. Magn., vol. 53, no. 6, pp. 1–4, Jun. 2017, DOI: 10.1109/TMAG.2017.2661401.
- [24] "IEC60034: Rotating electrical machines - Part 18-41: Partial discharge free electrical insulation systems (Type I) used in rotating electrical machines fed from voltage converters - Qualification and quality control tests," International Electrotechnical Commission, Standard, 2014.
- [25] D. Roger, S. Ait-Amar, and E. Napieralska, "A method to reduce partial discharges in motor windings fed by PWM inverter," Open Physics, vol. 16, no. 1, pp. 599–604, Oct. 2018, DOI: 10.1515/phys-2018-0078.
- [26] Z. Ren, "A 3D vector potential formulation using edge element for electrostatic field computation," IEEE Trans. Magn., vol. 31, no. 3, pp. 1520–1523, May 1995, DOI: 10.1109/20.376319.
- [27] "IEC60317-0-1: Specifications for particular types of winding wires – Part 0-1: General requirements – Enamelled round copper wire," Standard, 2008.
- [28] P. Collin, D. Malec, and Y. Lefevre, "About the relevance of using Paschen's criterion for partial discharges inception voltage (PDIV) estimation when designing the electrical insulation system of inverter fed motors," in Proc. EIC, Jun. 2019, pp. 513–516, DOI: 10.1109/EIC43217.2019.9046558.
- [29] L. Lusuardi, A. Cavallini, A. Caprara, F. Bardelli, and A. Cattazzo, "The Impact of Test Voltage Waveform in Determining the Repetitive Partial Discharge Inception Voltage of Type I Turn/Turn Insulation Used in Inverter-Fed Induction Motors," in Proc. EIC, Jun. 2018, pp. 478–481, DOI: 10.1109/EIC.2018.8481018.
- [30] L. Benmamas, P. Teste, F. Vangraefschepe, G. Krebs, E. Odic, T. Hamiti, and É. Berthelot, "Validation d'un modèle de bobinage par analyse fréquentielle et temporelle," in Proc. SGE, Grenoble, France, Jun. 2016.
- [31] M. Toudji, G. Parent, S. Duchesne, and P. Dular, "Determination of winding lumped parameter equivalent circuit by means of finite element method," IEEE Transactions on Magnetics, vol. 53, no. 6, pp. 1–4, Jun. 2017, DOI: 10.1109/TMAG.2017.2671423.



THÉO MATHURIN was born in Pontoise, France in 1992. He earned his Master in Science and Executive Engineering from MINES ParisTech in 2014, with a Minor in nuclear engineering. Working at the Institute for Micro and Nanotechnology, he later obtained a PhD in micromagnetism from Centrale Lille in 2017.

After his PhD, he worked as a science writer from 2017 to 2019. He is currently a research engineer at the Laboratoire Systèmes Électrotechniques et Environnement (LSEE) within Artois University in Béthune, France. His interests lie in computer simulation in physics and engineering as well as in software development for scientific and research applications.





STÉPHANE DUCHESNE was born in the north of France in 1977, he obtained his Master of Science from the University of Lille in 2000 and his PhD in 2004 at the Artois University. He has been a full professor at the electrical engineering department of the Artois University (LSEE - Laboratoire Systèmes Electrotechnique et environnement) since 2015. His research topics concern electrical machines operating in harsh operating conditions. He focuses especially on the electrical insulation system and its mechanisms of failure, its aging and the evaluation of its health status.



GUILLAUME PARENT was born in 1979 in Strasbourg (France). He received his B.S. and M.S. degrees in electrical engineering from the University of Lille (France) in 2004 and the Ph.D. degree in electrical engineering from both the University of Lille and the University of Liège (Belgium) in 2008.

From 2008 to 2010, he was a Research Assistant with Laboratoire d'Électrotechnique et d'Électronique de Puissance (L2EP) in the École Centrale de Lille (France). From 2010 to 2019, he was an Assistant professeur with the Laboratoire Systèmes Électrotechnique et Environnement (LSEE) in the Artois University (France). Since 2019, he is a Full Professor with the LSEE. His main research interests include electromagnetic analysis with the finite element method applied to electromagnetic devices design.

• • •